Build Simul (2024) 17: 543–560
https://doi.org/10.1007/s12273-023-1098-x

Potential application of radiant floor cooling systems for residential buildings in different climate zones

Mengying Cui[1], Yang Song[1], Yudong Mao[1], Kaimin Yang[1], Jiying Liu[1] (✉), Zhe Tian[2,3] (✉)

1. School of Thermal Engineering, Shandong Jianzhu University, Jinan 250101, China
2. School of Environmental Science and Engineering, Tianjin University, Tianjin 300072, China
3. Key Lab of Building Environment and Energy of Tianjin, Tianjin University, Tianjin 300072, China

Abstract

A radiant floor cooling system (RFCS) is a high-comfort and low energy consumption system suitable for residential buildings. Radiant floor systems usually work with fresh air, and their operating performance is affected by climatic conditions. Indoor and outdoor environmental disturbances and the system's control strategy affect the indoor thermal comfort and energy efficiency of the system. Firstly, a multi-story residential building model was established in this study. Transient system simulation program was used to study the operation dynamics of three control strategies of the RFCS based on the calibrated model. Then, the performance of the control strategies in five climate zones in China were compared using multi-criteria decision-making in combination. The results show that control strategy has a negligible effect on condensation risk, but the thermal comfort and economic performance differ for different control strategies. The adaptability of different control strategies varies in different climate zones based on the consideration of multiple factors. The performance of the direct-ground cooling source system is better in Hot summer and warm winter zone. The variable air volume control strategy scores higher in Serve cold and Temperate zones, and the hours exceeding thermal comfort account for less than 3% of the total simulation period. Therefore, it is suggested to choose the RFCS control strategy for residential buildings according to the climate zone characteristics, to increase the energy savings. Our results provide a reliable reference for implementing RFCSs in residential buildings.

Keywords

control strategy
radiant floor cooling system
residential building
energy efficiency
climate zones

Article History

Received: 05 October 2023
Revised: 07 November 2023
Accepted: 28 November 2023

1 Introduction

Building energy conservation and emission reduction require improvements, especially with the increase in the building area. Building cooling comprises a large proportion in building energy consumption due to climate warming and increased energy demands. Higher cooling energy consumption during summer would strain the grid (Delmastro et al. 2022). Radiant cooling systems were first used in Europe and have since developed rapidly (Bean et al. 2010), with numerous successful applications in residential buildings (Kalz et al. 2010; Hu and Niu 2012), office buildings (Joe et al. 2018), airports (Zhao et al. 2016), and other structures. Radiant floor cooling system (RFCS) utilizes radiant heat exchange between a radiant surface and other surfaces (human body, furniture, and enclosure structures) for cooling. This system can create of comfortable indoor conditions and utilize natural cold sources for cooling while minimizing primary energy usage (Rhee et al. 2017). The direct-ground cooling systems using natural cold sources have been widely applied. They utilize the shallow geothermal energy for cooling indoor spaces (Hou et al. 2018). However, RFCSs would be not suitable for short-term load changes, although the storage capacity of buildings can be used for the load transfer by the system (Tian and Love 2009; Sui et al. 2020).

Reasonable control of RFCSs can reduce the influence of internal and external disturbance on the indoor thermal environment and reduce energy consumption. Numerous

E-mail: JXL83@sdjzu.edu.cn (Jiying Liu); tianzhe@tju.edu.cn (Zhe Tian)

List of symbols

A	building area (m^2)
C_p	annual carbon reduction by carbon sink system of building green space ($kgCO_2/m^2$)
EF_i	carbon emission factor
$E_{i,j}$	annual consumption of building energy (unit/a)
H_{cons}	condensation risk hour (h)
H_{disc}	discomfort hour (h)
h_c	heat exchange coefficient by convection ($W/(m^2 \cdot K)$)
h_r	heat exchange coefficient by radiation ($W/(m^2 \cdot K)$)
i	iteration number
m_i	calibrated data
$\overline{m}$	average value
PD	percentage dissatisfied (%)
$\hat{s}_i$	predicted data
T_{idew}	dew point temperature (°C)
T_{in}	indoor air temperature (°C)
T_{iset}	indoor air temperature set-point (°C)
T_{out}	outdoor air temperature (°C)
T_r	radiant temperature (°C)
T_f	floor surface temperature (°C)
T_{sa}	supply air temperature (°C)
T_{sw}	supply water temperature (°C)
V_0	minimum supply airflow (m^3/h)
V_{sa}	supply airflow (m^3/h)
y	design life of the building (a)

Abbreviations

ACH	air change rate (h^{-1})
CEs	carbon emissions ($kgCO_2/m^2$)
CR	condensation risk
EC	energy consumption (kWh/m^2)
EH_p	uncomfortable hours indoors during working hours (h)
EH_r	total hours with condensation risk of the radiant floor (h)
HSCW	hot summer and cold winter zones
HSWW	hot summer and warm winter zones
SC	severe cold zones
TC	thermal comfortable
WB	wet bulb temperature (°C)

Subscripts

a	indoor air
c	convection
idew	indoor dew point
i	type of terminal energy consumed by the building
iset	set-point
j	type of building energy consumption system
r	radiation
f	radiant cooling surface
sa	supply air
sw	supply water

control strategies for RFCS have been investigated. Gwerder et al. (2009) proposed a pulse width modulated intermittent operation for a water circulation pump, considering the uncertainty of load disturbance. The system was in line with the comfort standard and was energy efficient. Pulse width modulated intermittent control reduces the power demand of circulating pumps by more than 50% compared to continuous operation (Lehmann et al. 2011). Schmelas et al. (2017) developed an adaptive prediction method based on multiple linear regression, significantly reducing pump running time and investment costs (Schmelas et al. 2015). Zakula et al. (2015) used a predictive model for heuristic feedback control in radiant floor integrated ventilation system to optimize the control for the next 24 hours based on weather and load prediction. The study found that RFCS had 50% lower electrical energy consumption than traditional variable air volume system and reduced the peak power load by 74%. Despite the effectiveness of advanced control strategies, conventional control strategies are also being improved. Intermittent control based on weather forecasting enables the response to changes in the indoor thermal environment in advance, lowering building energy consumption (Liu et al. 2019). It is crucial to select the appropriate cooling time for intermittent control. Furthermore, integrating supply water temperature control can substantially mitigate indoor temperature fluctuations (Sui et al. 2020). The choice of control strategy is significant for the operation of RFCSs.

Climatic conditions can affect the performance of RFCS (Vivek and Balaji 2023), particularly in high-humidity climate zones with an increased condensation risk on the radiant system. Condensation can result in higher dehumidification energy requirements. Srivastava et al. (2018) analyzed the operational performance of RFCS consisting of evaporative cooling and a chiller in various climate types in India. It was found that the energy-saving potential of the RFCS was limited in warm and humid climate. A suitable control strategy was required to improve the system's efficiency. Salvalai et al. (2013) used transient system simulation program (TRNSYS) to compare the effects of radiant cooling system in six European climates. It was found that the radiant cooling systems provided superior

thermal comfort compared to air systems. Although the energy conservation efficiency of RFCSs differs in different climates, the system is suitable for different climate types (Li et al. 2018).

The RFCSs in China face various challenges due to the diverse climate zones (Zhang et al. 2021). The design of RFCSs is complex, requiring extensive research to understand the various influencing factors and patterns, especially the indoor thermal environment impact cost. Although many studies have focused on innovative control strategies and unilateral analysis, it remains crucial to conduct the comparative analyses of the RFCS performance, especially considering the effects of different climates. This study focuses on residential building and analyzes the potential of RFCS in five climate zones in China. Firstly, three conventional control strategies for RFCS are proposed. The use of three control strategies in 11 cities in five climate zones is simulated in TRNSYS. Then, the indoor thermal comfort and economic efficiency of the control strategies are evaluated according to the simulation results. Finally, thermal comfort, condensation risk, energy consumption and carbon emissions are considered to select the optimal strategies for different cities.

2 Method

2.1 Building model and selection of climate zone

Due to the diverse climate types in China, significant temperature differences between northern and southern areas, and notable variations in humidity between eastern and western areas, China was divided into five climate zones based on temperature variations and practical building design: Serve cold (SC), Cold, Hot summer and cold winter (HSCW), Hot summer and warm winter (HSWW), and Temperate zones. Eleven cities in five climate zones were selected to simulate and explore the operational performance of an RFCS with three control strategies.

These cities include Shenyang in the SC zone, Xi'an, Beijing and Jinan in the Cold zone, Chengdu, Wuhan, and Shanghai in the HSCW zone, Nanning, Guangzhou, and Fuzhou in the HSWW zone, and Guiyang in the Temperate zone (Figure 1). The meteorological data source is Chinese standard weather data. The outdoor air temperature and relative humidity in the eleven cities from June to August are shown in Figure 2. The SC and Temperate zones have lower outdoor air temperature and relative humidity than other climate zones, requiring fewer cooling days. The HSCW and HSWW zones have higher temperature and humidity than other zones. Furthermore, the fluctuations in outdoor air relative humidity are smaller in the HSCW and HSWW zones than in the Cold zone.

The study focuses on a residential building, the room layout and building model are shown in Figure 3. There are two housing units on each floor, with the same layout across its 11 floors and each floor height of 3 m. The radiant floor system transfers cold energy using convective and radiant heat transfer. The floor consists of floor layer, insulation

Fig. 1 Location of 11 cities used in this study (GS 京(2024)0318)

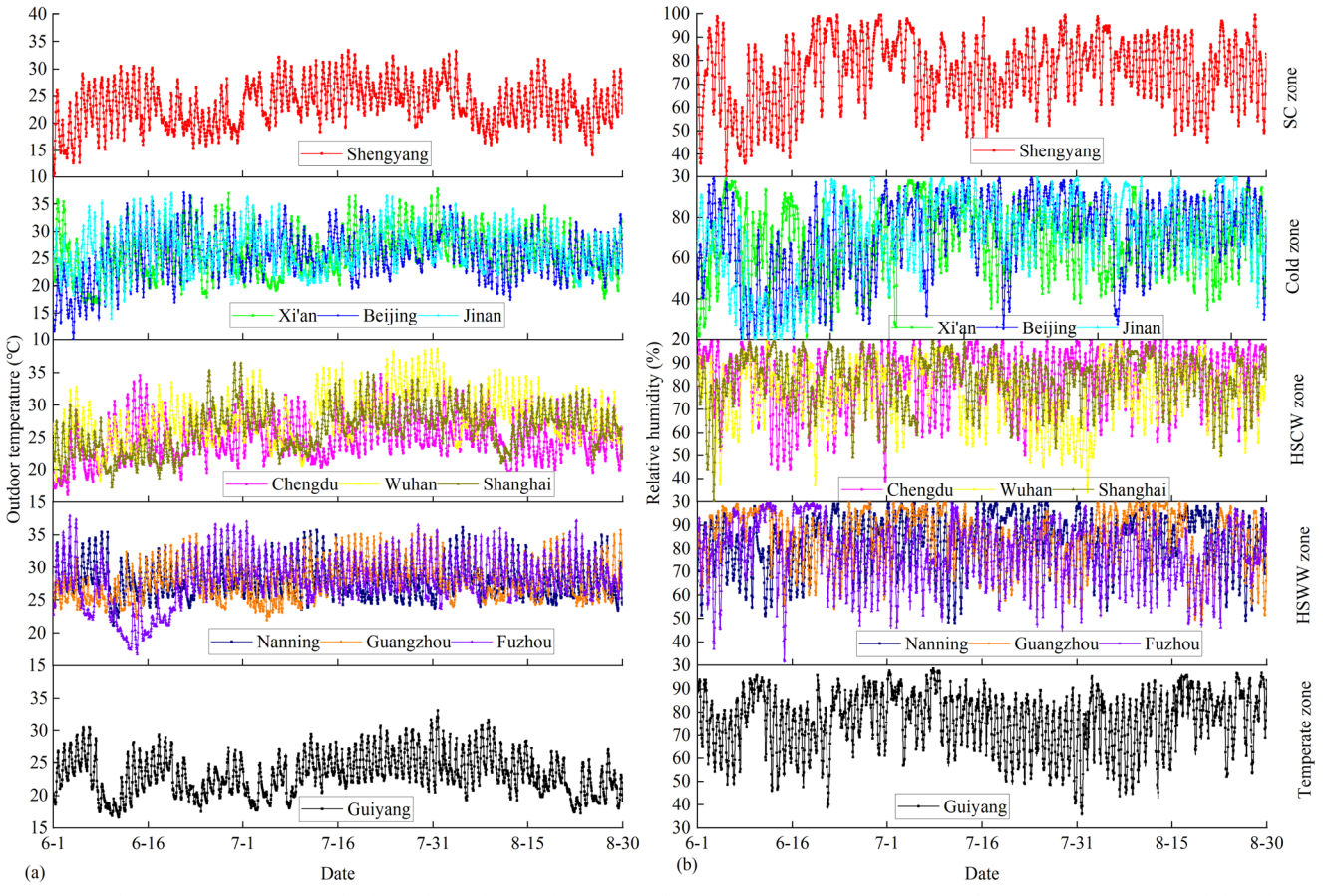

Fig. 2 Outdoor air temperature and relative humidity in eleven cities from June 1 to August 30: (a) outdoor air temperature, and (b) relative humidity

layer, buried pipe layer, screed layer, and surface layer (Figure 3). The parameters of the floor are listed in Table 1. The heat transfer coefficient of the building envelopes and the indoor heat gains in the five climate zones are set based on the GB 55015-2021 standard (MOHURD 2021) (Table 2). Three people were assumed to live in a household and the household occupancy schedule is shown in Figure 3(d). When all people were present, each person generated 61 W of sensible heat and emitted 109 g/h of moisture. The metabolic rate was 1.2 met, and the clothing insulation was 0.5 clo of clothing. A room in the middle of the unit was used in the simulation to minimize the influence of external factors. The sensible heat, latent heat load and load proportion of the building in different cities are shown in Figure 4. Shenyang has the largest building load, followed by Wuhan, and Guiyang has the smallest building load. The latent heat load constitutes more than 50% of the total load in most cities. The latent heat load has a larger proportion in the HSCW and HSWW zones and the latent heat load in Wuhan accounts for 66.8% of the total building load. Buildings in the SC and Temperate zones have lower proportions of the latent heat load than those in other zones. The building in Xi'an in the Cold zones has the smallest proportion of latent heat load, accounting for only 47.4% of the total building load.

2.2 Control strategies and system models

The diagram of the RFCS is shown in Figure 5. The RFCS includes a radiant floor system and a ventilation system, which operates continuously. According to the standard (MOHURD 2012), the lowest temperature of the floor in a room occupied by people is 19 °C. The heat pumps or direct-ground cooling sources are usually used to produce high temperature cooling water as the radiant floor system requirements. The ventilation system has composed of humidity control and temperature control systems. The ground source heat pump generates chilled water (7 °C) to cool and dehumidify the fresh air, after which the supply air temperature is adjusted by the temperature control. According to the standard (MOHURD 2018), the air volume is designed to be 0.5–1.5 h^{-1}, considering auxiliary cooling and dehumidification requirements. The control module performs adjustments based on the indoor environmental

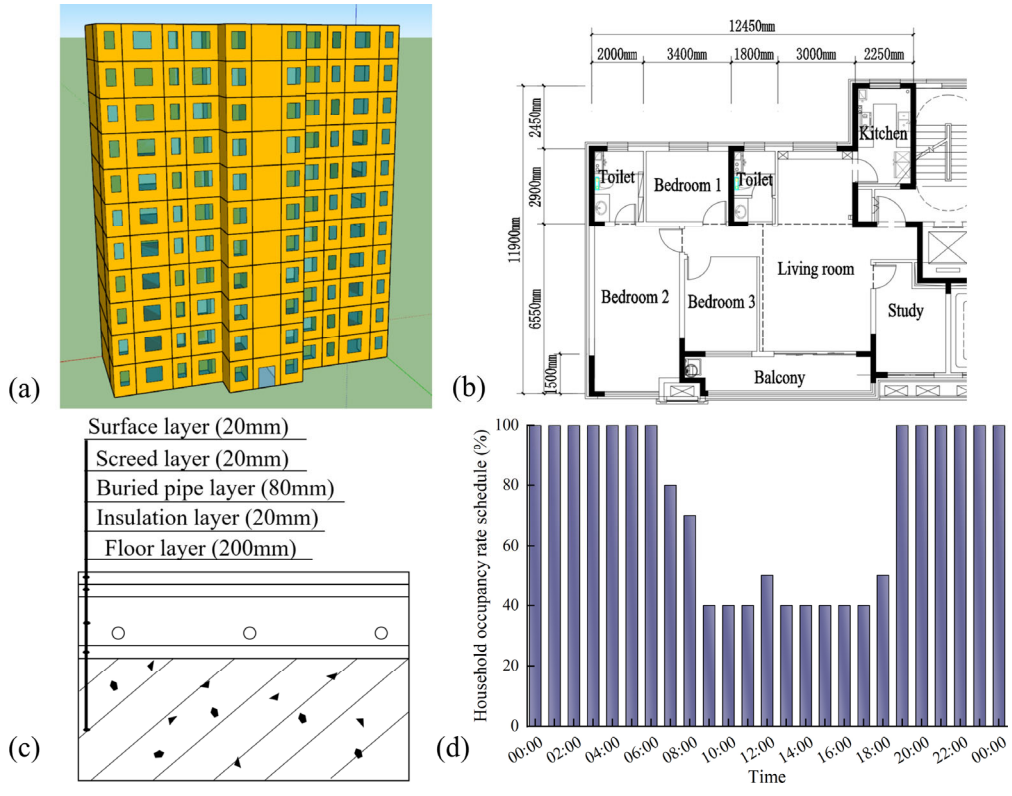

Fig. 3 Description of the residential building model: (a) 3D model of building stereogram, (b) floor plan, (c) radiant floor structure composition, and (d) household occupancy schedule

Table 1 Parameters of the radiant floor

Category	Thickness (mm)	Material type	Density (kg/m^3)	Thermal conductivity (W/(m·K))
Surface layer	20	Marble	2800	2.91
Screed layer	20	Cement mortar	1800	0.93
Buried pipe layer	120	Gravel concrete	2100	1.84
Insulation layer	20	Expanded polystyrene board	35	0.021
Floor layer	200	Concrete	2400	1.28

Table 2 Heat transfer coefficient of building envelopes in five climate zones

Climate zones	City	Heat transfer coefficient (W/(m^2·K))	
		Roof	Wall
SC	Shenyang	0.2	0.35
Cold	Xi'an, Beijing, Jinan	0.25	0.45
HSCW	Chengdu, Wuhan, Shanghai	0.4	1
HSWW	Nanning, Guangzhou, Fuzhou	0.4	1.5
Temperate	Guiyang	0.4	1

parameters and regulates the supply water temperature, supply water flow rate, air supply temperature, and air supply volume of the RFCS.

Three strategies were investigated (Figure 6): variable water temperature control, variable air volume control and direct-ground source cooling. The parameter for the three control strategies is presented in Table 3.

Variable water temperature control (Strategy 1): Strategy 1 controls the water supply temperature, the ON/OFF operation of the radiant floor system, and the air supply volume of the ventilation system. Proportional mixing of the supply and return water is employed to adjust the water supply temperature. The water supply temperature of the radiant floor system is adjusted according to the indoor air temperature. This adjustment includes reducing the water supply temperature when the air temperature exceeds T_{iset} + 1, maintaining the water supply temperature when the air temperature is in the range of T_{iset} − 1 to T_{iset} + 1, and increasing the water supply temperature when the air temperature is below T_{iset} − 1. The supply water temperature of the radiant floor system ranges from 16 to 19 °C and is

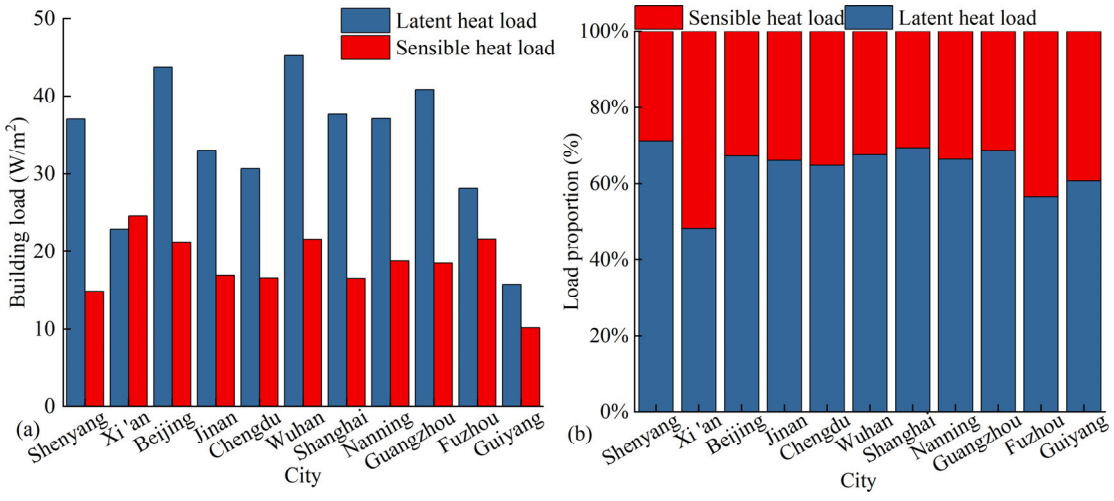

Fig. 4 Information for the building load: (a) comparison of latent heat load and sensible heat load, and (b) load proportion

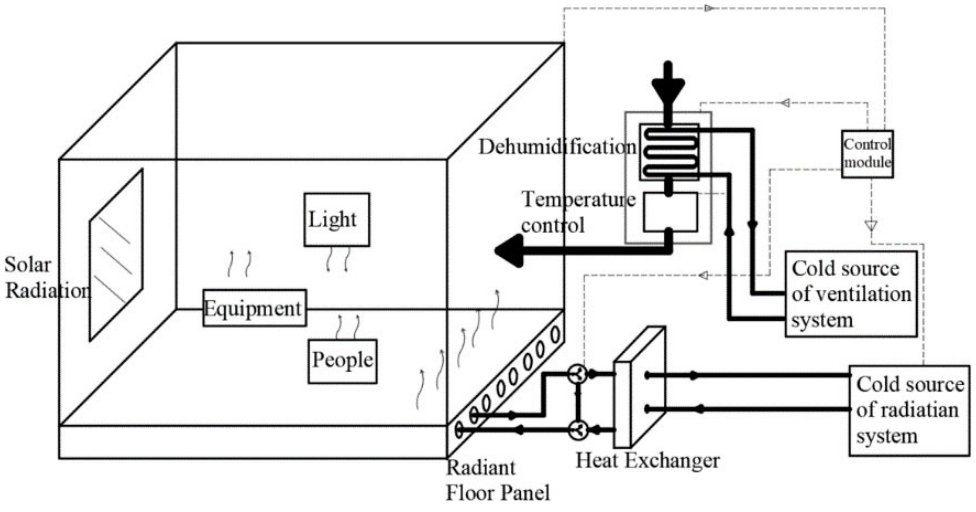

Fig. 5 Schematic diagram of RFCS

Table 3 Parameters of different control strategies

Control strategy		Strategy 1	Strategy 2	Strategy 3
Monitoring variables		T_{in}, T_{idew}, T_f, T_{sw}	T_{in}, T_{idew}, T_f	T_{in}, T_{idew}, T_f
Ventilation system	Supply air temperature (°C)	24	24	22/24
	Air change rate (h^{-1})	0.5–1.2	0.5–1.5	0.5–1.5
	Cold source	Ground source heat pump		
Radiant floor system	Supply water temperature (°C)	16–19	18	18.5–20
	Cold source	Ground source heat pump		Direct-ground cooling source
Simulation period		SC and Temperate zones: June 15–Sep. 15; Cold, HSCW and HSWW zones: May 1–Sep. 30		

adjusted in increments of 1 °C, accelerating cooling of the floor in overheated environments. The supply air temperature of the ventilation system is 24 °C and the supply air volume is increased when condensation risk of the radiant floor surface exists. The risk of condensation occurs in the strategy when $T_f - T_{idew} \leq 2$ °C.

Variable air volume control (Strategy 2): Strategy 2 uses the ventilation system to adjust the indoor environment, perform the ON/OFF control of the radiant floor system, and regulate the supply air volume. The ventilation system can handle a higher indoor load and respond quickly to changes in the indoor load. The supply air temperature is

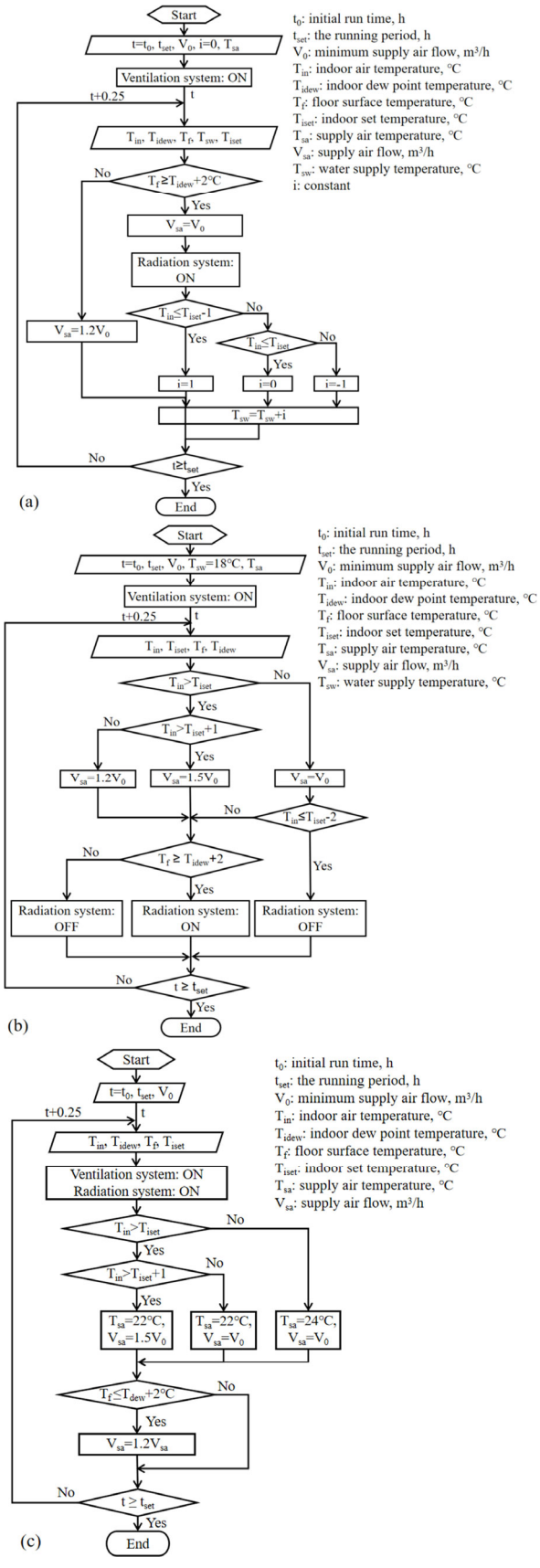

Fig. 6 Flow-charts of three strategies: (a) Strategy 1, (b) Strategy 2, and (c) Strategy 3

24 °C. When the air temperature exceeds T_{iset} + 1, V_{sa}=1.5V_0. When the air temperature is in the range of T_{iset} to T_{iset} + 1, and V_{sa} = 1.2V_0, while for all other cases, V_{sa} = V_0. Strategy 2 prevents condensation by controlling the radiant surface temperature. The radiant floor system is turned off when the risk of condensation on the radiant floor exists or the indoor air temperature is lower than T_{iset} − 1. Otherwise, the system is turned on. The water supply temperature of the radiant floor system is 18 °C.

Direct-ground source cooling (Strategy 3): Strategy 3 uses a direct-ground cooling source in conjunction with ventilation system to regulate the indoor environment. The cooling provided by the direct-ground cooling source fluctuates, resulting in variations in the supply water temperature within the range of 18.5 to 20 °C. Therefore, the radiant floor system operates throughout the day to maximize the cooling of the floor. This allows for pre-cooling the floor when the indoor load is low and cooling the room when the indoor load is higher. The ventilation system is adjusted to assist with cooling and dehumidification by regulating the supply air temperature and supply air flow rate. The supply air temperature is 22/24 °C and the airflow rate ranges from 0.5 to 1.5 h^{-1}. If T_{in} > T_{iset} + 1, the supply air temperature should be lowered, and the airflow rate should be increased simultaneously. The supply air volume is increased for dehumidification when T_f − T_{idew} ≤ 2 °C to mitigate condensation risk on the radiant surface.

The RFCSs are modularized and modeled using TRNSYS (Figure 7). Type56 is used as the parameter to import building parameter. Type155 is used to control the system. It accepts indoor environmental parameters and transmits control signals to water and air systems. The ventilation system consists of Type 508, Type 760, and Type 930. Type 760 in the ventilation system is utilized for energy recovery to reduce cooling energy consumption. The buffer tank keeps the water system stable and prevents frequent starting and stopping of the unit. As shown in Figure 7(a), Type 11 is used to adjust the mixing ratio of the supply and return water to achieve the desired water supply temperature. The step size was 0.25 h during the simulation.

2.3 Evaluation of control strategy

2.3.1 Indoor comfort evaluation

The thermal comfort of people is affected by various realistic conditions. Analyzing various parameters can provide a deeper understanding of the indoor thermal environment. This study considers the four aspects of thermal comfort: operative temperature (T_{op}), local thermal discomfort caused by warm and cool floors, predicted mean vote (PMV), and condensation risk. Indoor air temperature is

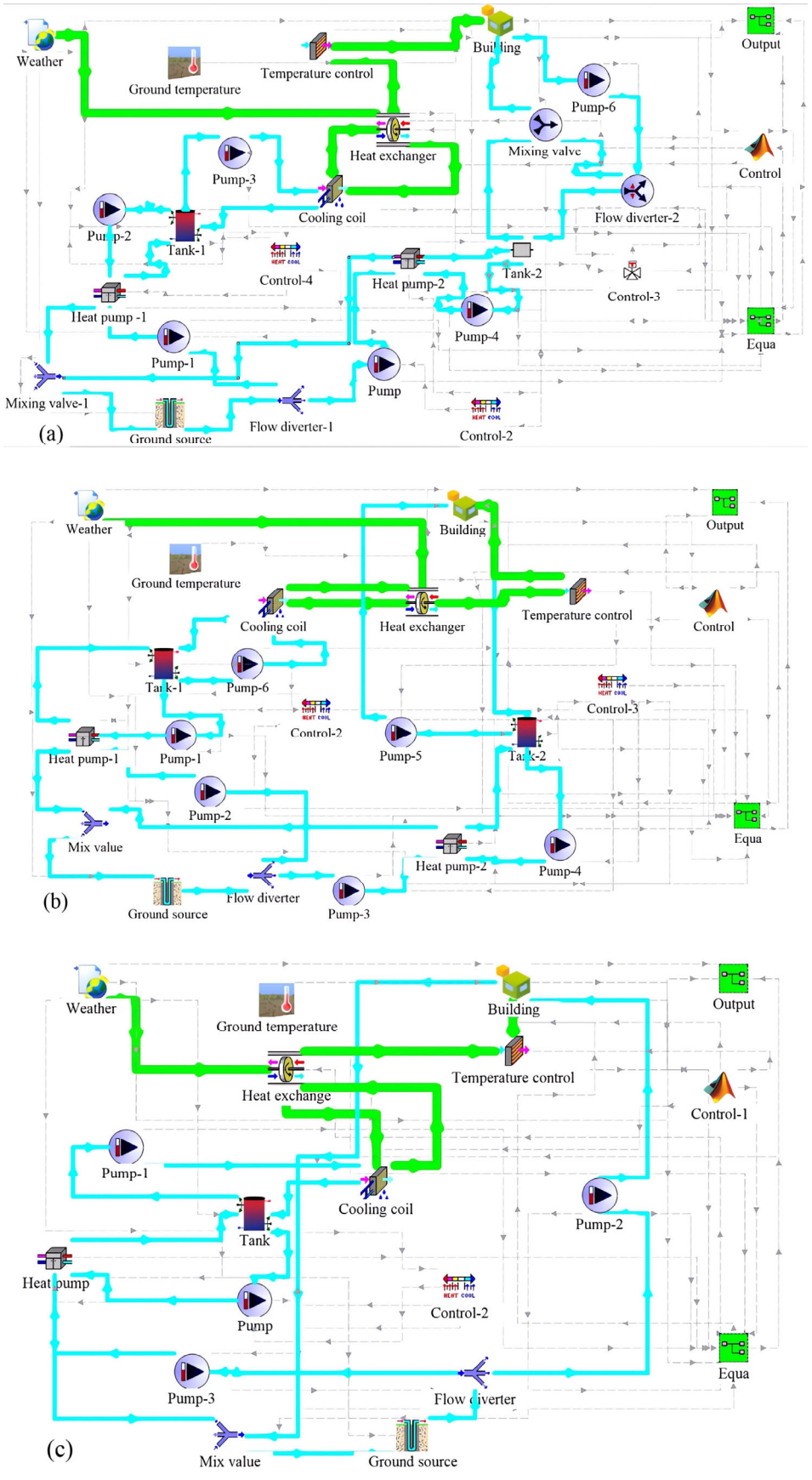

Fig. 7 The system model in TRNSYS for the three strategies: (a) Strategy 1, (b) Strategy 2, and (c) Strategy 3

a more intuitive thermal comfort parameter. The range recommended standards is 24–26 °C (MOHURD 2021). However, rooms equipped with an RFCS can still achieve good thermal comfort at temperatures above 26 °C. This is because the air temperature fails to consider the impact of radiative heat transfer. Therefore, T_{op} is given more consideration. It is calculated using Equation (1) (ASHRAE 2014).

$$T_{op} = \frac{h_c T_{in} + h_r T_r}{h_c + h_r} \tag{1}$$

where T_{in} is the indoor air temperature; T_r is the indoor mean radiant temperature; h_c is the convective heat transfer coefficient; h_r is the radiation heat exchange coefficient.

The floor surface temperature could remain too cold in neutral thermal conditions, causing local thermal discomfort. Therefore, the local thermal discomfort caused by cold floors is considered by evaluating the indoor thermal comfort environment. The equation of percentage dissatisfied due to warm or cold floors is defined using Equation (2). The maximum value is 10% (ASHRAE 2014).

$$\mathrm{PD} = 100 - 94 \cdot \exp\left(-1.387 + 0.118 \cdot T_f - 0.0025 \cdot T_f^2\right) \tag{2}$$

where PD is the percentage dissatisfied; T_f is the floor temperature.

The PMV model is widely used as an evaluation index and a control target. When the PMV is within the range of −0.5 to 0.5, the indoor environment is neutral. The duration of time spent outside the thermal comfort range was calculated to assess the indoor environment during the cooling cycle. It is given by Equation (3) (ASHRAE 2014).

$$\mathrm{EH_p} = \sum H_{disc} \tag{3}$$

where $\mathrm{EH_p}$ is the exceedance hours of the PMV comfort zone; H_{disc} is a discomfort hour (H_{disc} = 1 if $|\mathrm{PMV}| - 0.5 > 0$ and 0 otherwise).

Radiant floor systems installed in the occupied area are prone to condensation, which adversely affects human comfort and system performance. Therefore, the condensation risk of the radiant surface is an important indicator of the RFCS. The condensation can be effectively prevented by controlling the surface temperature of the floor and the indoor air temperature. Condensation risk of the radiant floor is determined when $T_f - T_{idew} \le 2$ °C (Oxizidis and Papadopoulos 2013). The number of hours with condensation risk is evaluated to monitor the long-term operation of radiant floor. Similar to the evaluation of the PMV, the number of hours with condensation risk for radiant floor can be expressed using Equation (4). A high number of hours with condensation risk indicates ineffective management of the latent heat load in the room, indicating that the system has low adaptability in hot and humid climates. Relatively few hours with condensation risk implies that the latent heat load of the room can be effectively managed, indicating that the system has great potential for application in hot and humid climates.

$$\mathrm{EH_r} = \sum H_{cons} \tag{4}$$

where $\mathrm{EH_r}$ is the total hours with condensation risk of the radiant floor; H_{cons} is an hour with condensation risk of the radiant floor (H_{cons} = 1 if $T_f - T_{idew} \le 2$ °C and 0 otherwise).

2.3.2 *Economic evaluation*

The energy consumption, carbon emissions, and electricity cost of cooling for RFCS are evaluated. The total energy consumption of the RFCS is obtained for different control strategies in the simulation. The operating cost of the system is an essential metric for assessing the practical feasibility of implementing the system. The operating costs of the system are based on the electricity prices of different cities, which are shown in Table 4. Some cities define peak-valley electricity prices, such as Xi'an, Jinan, Shanghai, and Guangzhou, whereas others use constant price, creating gaps in system operating costs. The environmental impact of RFCS with different strategies is analyzed by comparing of carbon emissions, which are calculated by the standard GB/T51366-2019 (MOHURD 2019). The total carbon emissions per unit building can be calculated using Equations (5) and (6), where the carbon emission factor is determined based on the carbon emission source.

$$\mathrm{CEs} = \frac{\left[\sum_{i=1}^{n}\left(E_i \mathrm{EF}_i\right) - C_p\right] y}{A} \tag{5}$$

$$E_i = \sum_{j=1}^{n}\left(E_{i,j} - \mathrm{ER}_{i,j}\right) \tag{6}$$

where CEs is the carbon emissions per unit of building area during the building's operating stage; E_i is the annual energy consumption of building for Class i; EF_i is the CEs factor of the ith energy type; $E_{i,j}$ is the Class i energy consumption for Class j systems; $\mathrm{ER}_{i,j}$ is the amount of Class i energy supplied by a renewable energy system consumed by the Class j system; i is the type of terminal energy consumed by the building; j is the type of building energy consumption system, including heating, ventilation, and air conditioning (HVAC), and lighting; C_p is the annual carbon reduction attributed to the carbon sink system of the green space within the building premises; y is the design life of the building; A is the building floor area.

Table 4 Electricity prices in different cities

City	Electricity prices (yuan/kWh)
Shenyang	0.5000
Xi'an	Peak time (8:00–11:30, 18:30–23:00): 0.5400 Valley time (23:00–7:00): 0.2900 Remaining time (7:00–8:00, 11:30–18:30): 0.4900
Beijing	0.4773
Jinan	Peak time (8: 00–22: 00): 0.5769 Valley time (22: 00–8: 00): 0.3769
Chengdu	0.5464
Wuhan	0.5800
Shanghai	Peak time (6: 00–22: 00): 0.617 Valley time (22: 00–6: 00): 0.307
Nanning	0.5491
Guangzhou	Peak time (10: 00–12: 00, 14: 00–19: 00): 0.9863 Valley time (0: 00–8: 00): 0.2205 Remaining time (8: 00–10: 00, 12: 00–14: 00, 19: 00–00: 00): 0.5802
Fuzhou	0.5330
Guiyang	0.482

2.3.3 *Comparison of different strategies*

The evaluation that uses multiple indexes provide comprehensive evaluation of the RFCSs with different strategies. Thus, multi-criteria decision-making was used to assess and choose the optimal option. The evaluation procedure for multi-criteria decision making has been described in detail by Cui et al. (2023). The decision-making hierarchy is shown in Figure 8. It consists of three layers. The four criteria were thermal comfort, condensation risk, energy consumption and carbon emissions. At the bottom level are three control strategies. The alternatives were compared pairwise, and the results were assigned scores on a 9-point scale (Shahrestani et al. 2012). Then, the arithmetic mean was used to calculate the weight of each alternative. A comparison matrix was constructed, and subjective and objective priority weights were assigned. The RFCS with the highest overall score was selected after comparing the simulation results for various strategies. Table 5 lists the weight assignments for the criteria.

2.4 Simulation validation

Experiments were conducted on an experimental platform to validate the accuracy of the simulation (Figure 9). The laboratory comprised a radiant floor system integrated with a fan coil system. It included a control system, an indoor and outdoor environmental monitoring system. During the experiment, the air source heat pump provided chilled water for the system, which was then stored in a water tank. The experiment was designed to simulate residential

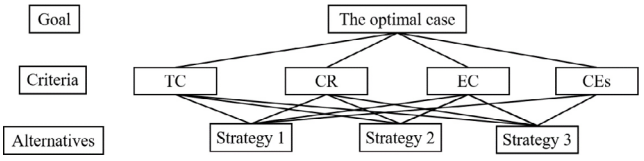

Fig. 8 The decision-making hierarchy (thermal comfort (TC), condensation risk (CR), energy consumption (EC), and carbon emissions (CEs))

Table 5 Three decision-making scenarios to select a radiant floor system (Cui et al. 2023; reprinted with permission ©2023 Elsevier)

Scenario	TC	CR	EC	CEs
1	0.25	0.25	0.25	0.25
2	0.15	0.15	0.25	0.45
3	0.25	0.45	0.15	0.15

buildings operating from 18:00 to 8:00 with an indoor heat gain. The RFCS was intermittently controlled and turned on two hours in advance. The indoor setpoint temperature was 26 °C.

The temperature of supply water of the radiant system was 2 °C higher than the indoor dew point temperature to prevent condensation. A mixed water pump was used in the system. More details on the experiment has been described by Zhu et al. (2022). The validation experiment was based on data August 2023, and calibration was performed using the data recorded in the operating system and the measured indoor parameters. The coefficient of variation of the root mean square error (CV-RMSE) and the normalized mean bias error (NMBE) were utilized to assess the accuracy of the simulation model. They were calculated respectively using Equations (7) and (8) (ASHRAE 2014). The values should meet the standard requirements: $|\text{NMBE}| \leq 5\%$, $\text{CV-RMSE} \leq 15\%$ (ASHRAE 2014).

$$\text{CV-RMSE} = \frac{\left[\sum_{i=1}^{n}\left(m_i - \hat{s}_i\right)^2 / \left(n-p\right)\right]^{\frac{1}{2}}}{\overline{m}} \times 100 \tag{7}$$

$$\text{NMBE} = \frac{\sum_{i=1}^{n}\left(m_i - \hat{s}_i\right)}{\left(n-p\right)\times\overline{m}} \times 100 \tag{8}$$

where m_i is the calibrated data; $\hat{s}_i$ denotes the predicted data; $\overline{m}$ is the average value ; n is the number of data; p equals 1.

The comparison of the measured and simulated results is presented in Figure 10. The simulated values of indoor temperature and relative humidity exhibit similar trends to the experimental values. The NMBEs for indoor air temperature and relative humidity are −0.30% and −0.02%, respectively, and the CV-RMSEs are 2.05% and 2.77%, respectively. The energy consumption of the system, is in the range of 11.2–13.2 kWh and 12.15–12.6 kWh in the

Fig. 9 Laboratory and instrument layout: (a) schematic diagram of laboratory and (b) schematic diagram of the field test in the laboratory

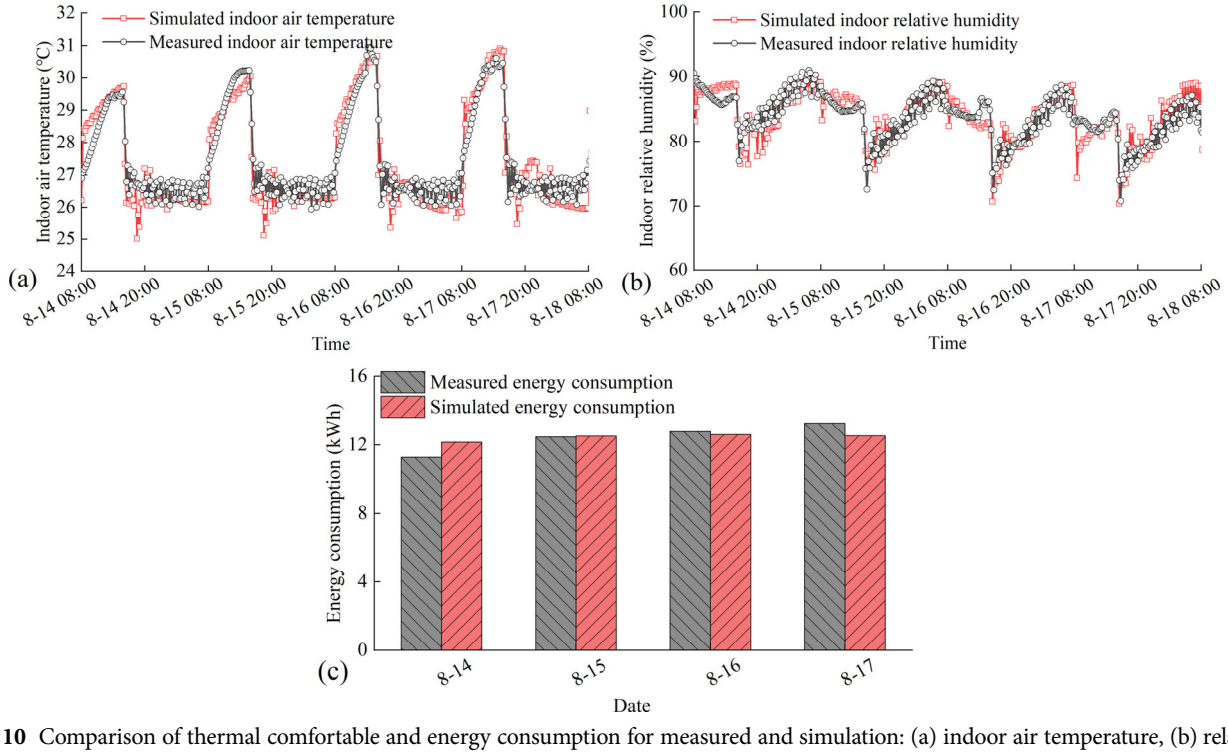

Fig. 10 Comparison of thermal comfortable and energy consumption for measured and simulation: (a) indoor air temperature, (b) relative humidity, and (c) energy consumption

experiments and simulations, respectively. The errors between model and experimental results exhibit relatively small, which can be attributed to factors such as instrument accuracy and idealized simulation settings. However, the errors fall within an acceptable range. Therefore, the validation confirms that the model possesses sufficiently high accuracy.

3 Results

3.1 Thermal comfort

3.1.1 Thermal comfort analysis

Wuhan (a city with high temperatures and humidity, as described in Section 2.1) was selected to highlight the characteristics of indoor parameter response. Figure 11 presents the values of the indoor parameters of three strategies in Wuhan from July 22 to July 29. The average T_{op} is 25.5 °C for Strategy 1, and 25.2 °C for Strategy 2, and 24.3 °C for Strategy 3. As the outdoor temperature increases, the T_{op} of Strategy 3 is gradually higher than that of the other two strategies after July 25. Among them, T_{op} fluctuation of Strategy 2 is the least. The PMV trend is similar to that of T_{op} due to indoor and outdoor conditions and exceeds the range of −0.5 to 0.5 in some periods. The PMV of Strategy 3 can reach 0.7. This result suggests that the cooling capacity of natural cold sources is limited. The relative humidity and the risk of condensation of the three strategies are influenced by the supply air volume and outdoor conditions. The indoor

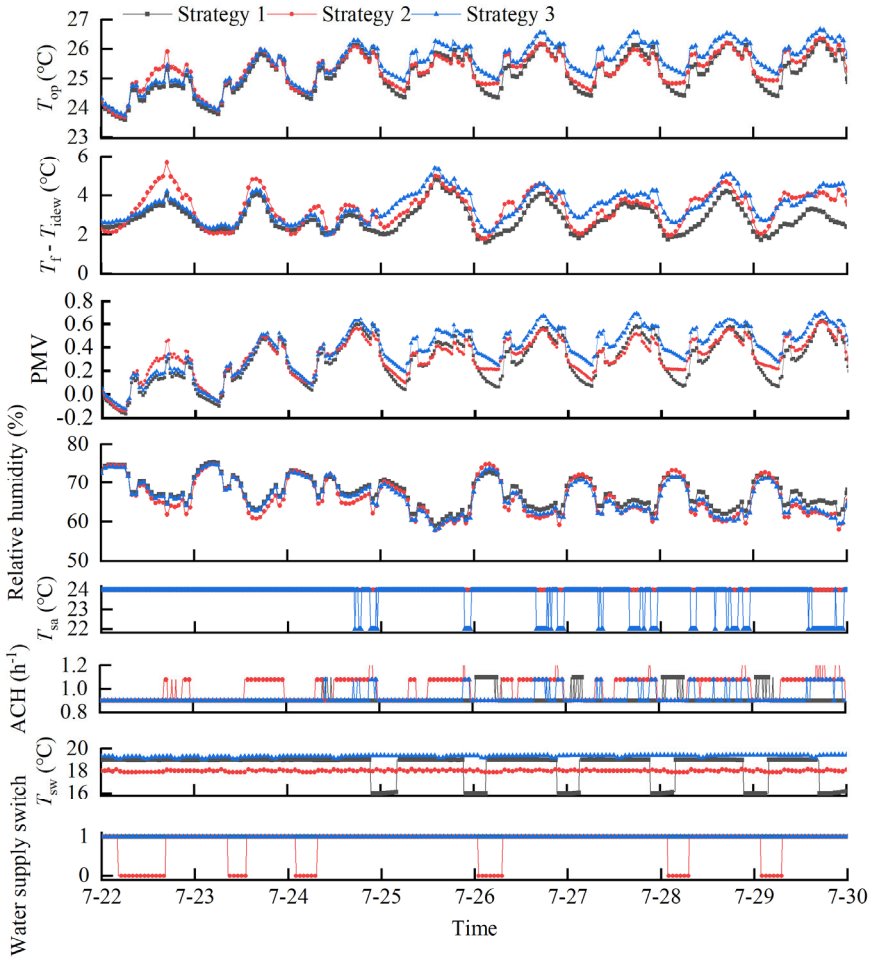

Fig. 11 Variations in indoor parameter values for three strategies in Wuhan

relative humidity ranges from 55% to 75%. The temperature difference is significantly lower at nighttime than during the daytime. The relative humidity of Strategy 1 is the highest; however, no condensation occurs on the floor surface. The control strategies can be effective in responding to changes in the indoor environmental parameters.

Figure 12 shows that the percentage distribution of dissatisfaction caused by warm or cold floors is less than 10%, indicating that the local thermal discomfort caused by cold floors is within the acceptable range. The percentage dissatisfied is relatively low in Strategy 2 compared to other strategies, while the difference distribution is relatively small in Strategy 3 (expect for Chengdu). The percentage distribution of dissatisfaction caused by warm floor and cold floor depends more on the strategy than the climate zone. Strategy 1 and Strategy 2 have the highest average percentage dissatisfied in the HSCW zone, whereas Strategy 1 has a higher average percentage dissatisfied in the HSWW zone.

The PMV of the three strategies in different cities from June to September is shown in Figure 13. The indoor thermal environment variations for different strategies exhibit similar trends in the same city. The indoor environment is cooler in the SC and Temperate zones and warmer in the Cold, HSCW and HSWW zones in July and August. In addition to overheating, a transitional period of supercooling also occurs. The number of hours exceeding the PMV comfort range in different cities is presented in Table 6. Strategy 3 shows significant fluctuations in the indoor PMV, with larger differences at the beginning, middle, and end of summer compared to the other two strategies, resulting in the longest duration of indoor heat discomfort. Strategy 1 performs slightly better than Strategy 3, with the hours of indoor thermal discomfort accounting for 6%–31% of the total simulated period in eleven cities. In Strategy 2, the indoor environment remains the most stable throughout the cooling period, with the fewest hours of thermal discomfort, constituting only 3% of the simulation period.

3.1.2 *Condensation risk analysis*

The risk of condensation on the surface of the radiant

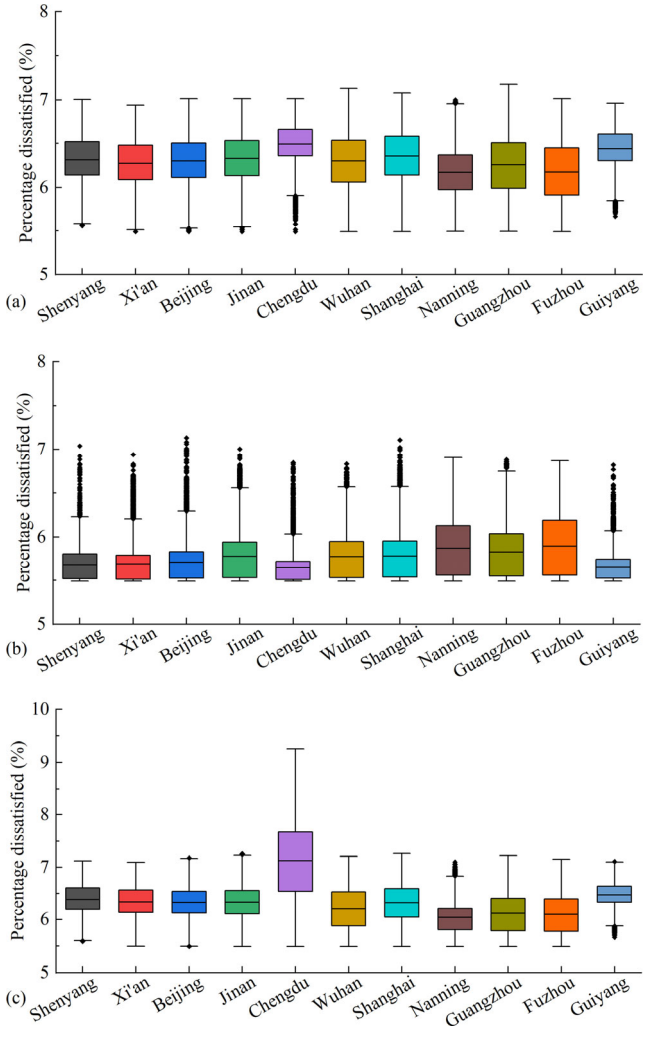

Fig. 12 Boxplots showing the distribution of percentage dissatisfied caused by warm or cool floors: (a) Strategy 1, (b) Strategy 2, and (c) Strategy 3

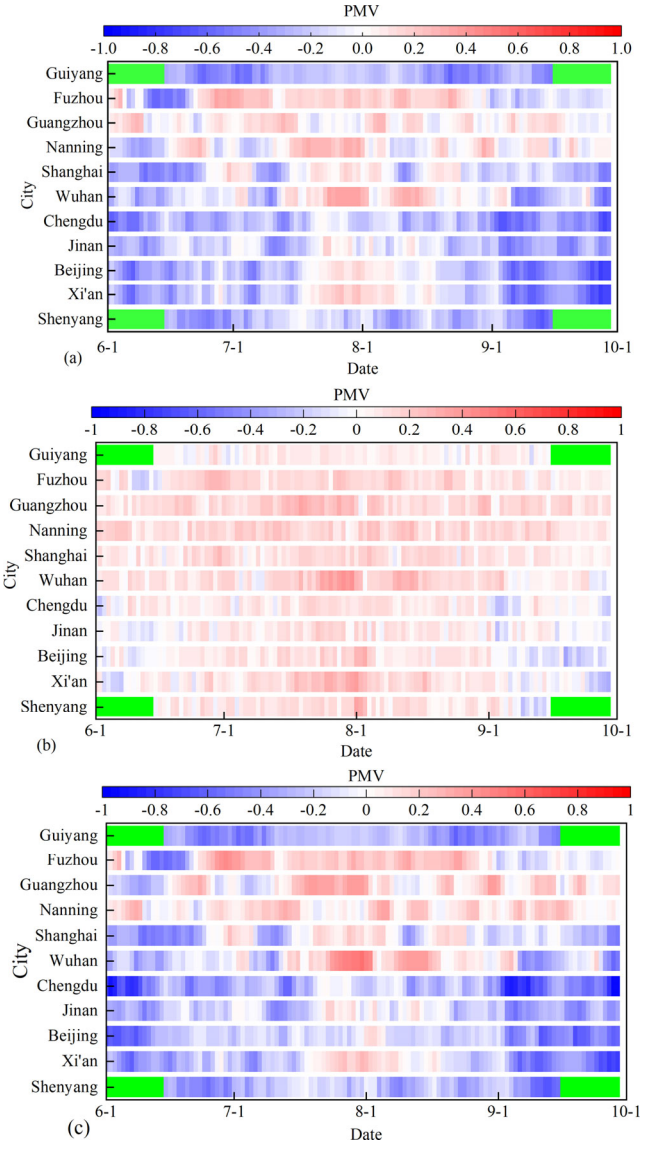

Fig. 13 Distribution of PMV for three control strategies in eleven cities (the part without simulation is shown in green): (a) Strategy 1, (b) Strategy 2, and (c) Strategy 3

floor can be effectively mitigated by the ventilation system. The condensation risk of the radiant floor is low in high-temperature and high-humidity conditions (Table 7). The risk is the highest in the HSWW zone, and the lowest in the Temperate zone. In RFCSs, the latent heat load is handled by the ventilation system. The number of hours with condensation risk occurs in the five climate zones is less than 10%. The condensation risk is the highest in the variable supply temperature control (Strategy 1), surpassing that of Strategy 3 by 19%. On average, the condensation risk hours account for 3% of the total simulation time. Strategy 1 has the highest risk of condensation in Nanning, and Strategy 3 has the highest condensation risk in Shenyang. Strategy 2 has the lowest number of condensation risk hours in the radiant floor system. The results indicate that it is critical to evaluate the condensation risk of different control strategies.

Table 6 The number of hours exceeding the comfort range of PMV

Climate zone	City	Strategy 1	Strategy 2	Strategy 3
SC	Shenyang	360	27	406
Cold	Xi'an	833	37	917
	Beijing	891	48	1004
	Jinan	630	25	679
HSCW	Chengdu	934	2	1510
	Wuhan	524	78	635
	Shanghai	583	5	624
HSWW	Nanning	48	12	63
	Guangzhou	23	7	117
	Fuzhou	359	11	441
Temperate	Guiyang	443	0	476

Table 7 The number of hours of condensation risk for the radiant floor system

Climate zone	City	Strategy 1	Strategy 2	Strategy 3
SC	Shenyang	150	48	225.5
Cold	Xi'an	68	56.75	118
	Beijing	53.25	20	48
	Jinan	25.75	26.25	11.5
HSCW	Chengdu	23.25	0.25	23.5
	Wuhan	112	72.75	53.75
	Shanghai	121.25	71.25	84.25
HSWW	Nanning	303	63.75	55.5
	Guangzhou	131.75	89.25	210.75
	Fuzhou	2.25	4	0.75
Temperate	Guiyang	0	0	0

3.2 Economic analysis

The energy consumption, electricity cost and carbon emissions of RFCS in different climate zones are compared in Figure 14 and Table 8. The energy consumption is the highest in the HSWW zone, followed by the HSCW, Cold, SC and Temperate zones. Strategy 3 uses a natural cooling source, which reduces most of the cooling energy consumption of the radiant floor system. The cooling energy consumption of Strategy 3 is 12.49 to 29.80 kWh/m^2, and the highest energy consumption occurs in Guangzhou.

Strategy 1 has a 19%–28% higher energy consumption than Strategy 3. However, Strategy 2 has a 3% lower energy consumption than Strategy 3 in the case of Chengdu. Although the carbon emissions and energy consumption trends are similar, the electricity costs differ for different cities due to electricity prices. The energy consumption of Nanning and Guangzhou is similar for the same strategy. The electricity cost is about 21% lower in Nanning than in Guangzhou (Figure 14). The electricity costs of different strategies in the same city are also influenced by peak-valley electricity prices.

3.3 Comprehensive comparison of the system

According to the simulation results, pairwise comparisons of the criteria for different control strategies were conducted. The arithmetic mean was used to determine the weights of the strategies (as shown in Table 9). The consistency ratio ranged from 0 to 0.1, indicating that all pairwise comparison matrices passed the consistency test. The ranking of the three control strategies in eleven cities was calculated based on the weights assigned to the strategies, as shown in Table 10. Strategy 3 does not consistently rank first in all cities in three scenarios, likely due to constraints related to exposure risk and thermal comfort. When it comes to preference for carbon emissions (Scenario 2), Strategy 3 with a natural cooling source ranks higher than the other strategies in eight cities, Strategy 2 ranks the highest in most cities in Scenario 1 and Scenario 3, followed by Strategy 3. In the comprehensive evaluation, Strategy 1 received the lowest score, which aligns with the other analysis results. Strategy 3 has a higher score in the HSWW zone, whereas Strategy 2 demonstrates advantages in the SC and Temperate zones.

4 Discussion

The application of RFCSs in residential building must consider the condensation risk and the response time (Kang et al. 2017; Ning et al. 2017). The dehumidification control of RFCSs is usually based on the condensation risk on the radiant surfaces (Zhu et al. 2022); thus, the indoor relative humidity may exceeding the specified range of 40%

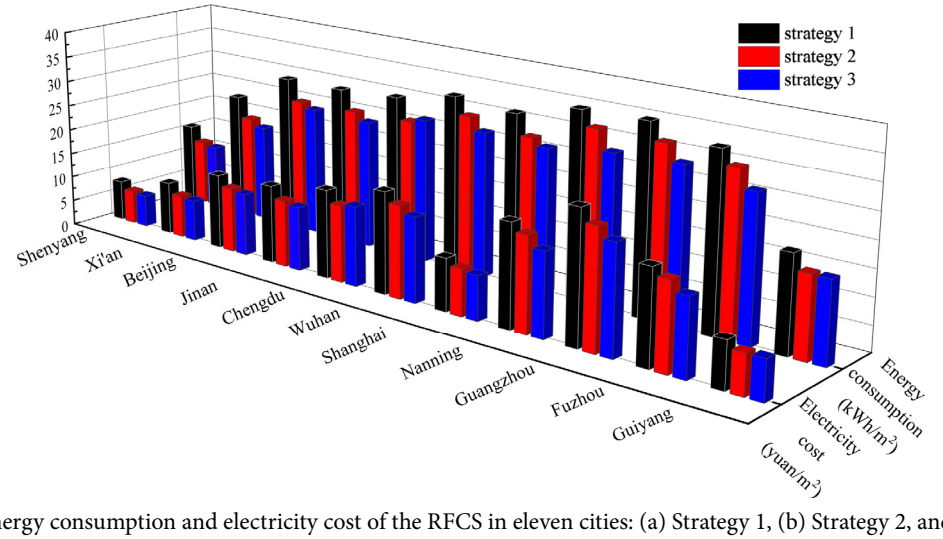

Fig. 14 The energy consumption and electricity cost of the RFCS in eleven cities: (a) Strategy 1, (b) Strategy 2, and (c) Strategy 3

Table 8 Cooling energy consumption and carbon emissions of the RFCS in eleven cities

City	Strategy 1		Strategy 2		Strategy 3	
	EC (kWh/m^2)	CEs ($kgCO_2/m^2$)	EC (kWh/m^2)	CEs ($kgCO_2/m^2$)	EC (kWh/m^2)	CEs ($kgCO_2/m^2$)
Shenyang	15.87	9.05	13.03	7.43	12.49	7.12
Xi'an	24.55	14.00	20.47	11.67	19.18	10.94
Beijing	30.52	17.41	26.30	15.00	25.31	14.43
Jinan	30.59	17.45	26.66	15.20	25.12	14.33
Chengdu	31.28	17.84	27.08	15.44	27.96	15.94
Wuhan	33.78	19.26	30.48	17.38	27.99	15.96
Shanghai	32.87	18.75	28.91	16.49	27.54	15.71
Nanning	35.96	20.51	33.00	18.82	29.24	16.68
Guangzhou	36.24	20.67	32.89	18.76	29.80	17.00
Fuzhou	33.91	19.34	31.16	17.77	27.56	15.72
Guiyang	18.52	10.56	15.68	8.94	15.57	8.88

Table 9 The weights of the criteria for the three control strategies in different cities

Climate zone	City	Strategy 1				Strategy 2				Strategy 3			
		CEs	EC	TC	CR	CEs	EC	TC	CR	CEs	EC	TC	CR
SC	Shenyang	0.099	0.094	0.191	0.206	0.374	0.344	0.692	0.723	0.527	0.562	0.117	0.070
Cold	Xi'an	0.072	0.067	0.105	0.365	0.313	0.316	0.815	0.503	0.615	0.617	0.080	0.132
	Beijing	0.072	0.068	0.118	0.250	0.313	0.345	0.808	0.500	0.615	0.587	0.074	0.250
	Jinan	0.072	0.067	0.105	0.286	0.313	0.294	0.789	0.286	0.615	0.640	0.105	0.429
HSCW	Chengdu	0.082	0.082	0.118	0.250	0.575	0.575	0.808	0.500	0.343	0.343	0.074	0.250
	Wuhan	0.072	0.067	0.163	0.155	0.239	0.244	0.740	0.504	0.689	0.689	0.097	0.342
	Shanghai	0.072	0.067	0.133	0.153	0.313	0.316	0.768	0.493	0.615	0.617	0.099	0.354
HSWW	Nanning	0.065	0.063	0.331	0.053	0.199	0.200	0.379	0.474	0.735	0.737	0.290	0.474
	Guangzhou	0.066	0.061	0.400	0.295	0.233	0.216	0.400	0.617	0.701	0.723	0.200	0.088
	Fuzhou	0.070	0.063	0.169	0.333	0.206	0.200	0.710	0.333	0.723	0.737	0.121	0.333
Temperate	Guiyang	0.111	0.100	0.091	0.333	0.444	0.450	0.818	0.333	0.444	0.450	0.091	0.333

Table 10 Ranking of the four strategies in different scenarios

Climate	City	Scenario 1	Scenario 2	Scenario 3
SC	Shenyang	2>3>1	2>3>1	2>3>1
Cold	Xi'an	2>3>1	3>2>1	2>3>1
	Beijing	2>3>1	3>2>1	2>3>1
	Jinan	3>2>1	3>2>1	2>3>1
HSCW	Chengdu	2>3>1	2>3>1	2>3>1
	Wuhan	3>2>1	3>2>1	2>3>1
	Shanghai	2>3>1	3>2>1	2>3>1
HSWW	Nanning	3>2>1	3>2>1	3>2>1
	Guangzhou	3>2>1	3>2>1	2>3>1
	Fuzhou	3>2>1	3>2>1	2>3>1
Temperate	Guiyang	2>3>1	2>3>1	2>3>1

to 60% (Zhou et al. 2022). The three control strategies result in higher indoor relative humidity than all-air systems, but no condensation occurred on the radiant surfaces. RFCSs are more tolerant of indoor relative humidity fluctuations, making it possible to allow some variation within a certain range. It is recommended to simultaneously control the temperature and humidity or incorporate dehumidification equipment to effectively maintain constant indoor temperature and humidity (Zarrella et al. 2014; Ren et al. 2022a). The average PMV values remain within an acceptable range during simulated periods of overheating. Among them, Strategy 2 exhibited the best thermal comfort effect and the lowest condensation risk, because it mainly regulates the ventilation system according to indoor and outdoor disturbances, and the system responds more quickly. More

hours with thermal discomfort occurred in Strategy 3, because it utilizes a direct-ground cooling source, reducing the peak indoor load through cold storage. Therefore, larger fluctuations in indoor thermal comfort conditions occur, and the control strategy requires improved control precision and system responsiveness (Schmelas et al. 2016).

The system that provided better thermal comfort was not the most energy-efficient system. Therefore, it is necessary to adjust the RFCS control strategy. In addition, the thermal comfort and energy consumption of the same strategy differed significantly in different cities. It is beneficial to adjust the set parameters or utilize the operative temperature or PMV as the control target to optimize the system (Ren et al. 2022b). Dehumidifiers may be more energy efficient than fresh air units in hot and humid climates. It is worth noting that intermittent control was more energy efficient than direct-ground cooling in Chengdu. Figure 15 shows the daily energy consumption and average PMV of the three control strategies in Chengdu. The continuous operation of RFCS can store energy for the building and results in energy consumption distribution (Abdel-Mawla et al. 2022). However, transmission energy consumption, an important aspect of energy saving efficiency, is increased (Lehmann et al. 2011). Although the natural cold source is conducive to reducing the energy consumption of the refrigeration system, in situations with higher indoor loads, the combination of mechanical cooling sources that improve the stability of the water supply is necessary (Chandrashekar and Kumar 2022). The indoor environment is the coolest at sometimes for Strategy 3, which means waste of energy.

The operational characteristics of RFCS with different strategies are similar in different building types, but comprehensive comparisons of research findings reveal significant differences (Li et al. 2018). The energy savings of radiant floor systems are higher in large buildings with comparable functions (Li et al. 2018), and natural cooling sources are more prevalent (Arghand et al. 2021; Cui et al. 2023). The overall building load of residential buildings is small, the latent load is large, and occupant behavior affects the load. Although the variable water temperature control did not exhibit advantages in terms of ranking or quantitative metrics in this study, it remains competitive in enhancing thermal comfort (Lim et al. 2006). A ventilation system can effectively supplement the cooling provided by the radiant system, but the proportion of its use affects the system's energy efficiency (Zhu et al. 2022).

The parameter setting of the conventional control strategies would affect the evaluation results. This study focused on the evaluation of control strategies but not on their optimization. In residential buildings, the dynamic behavior of occupants introduces uncertainty, affecting the

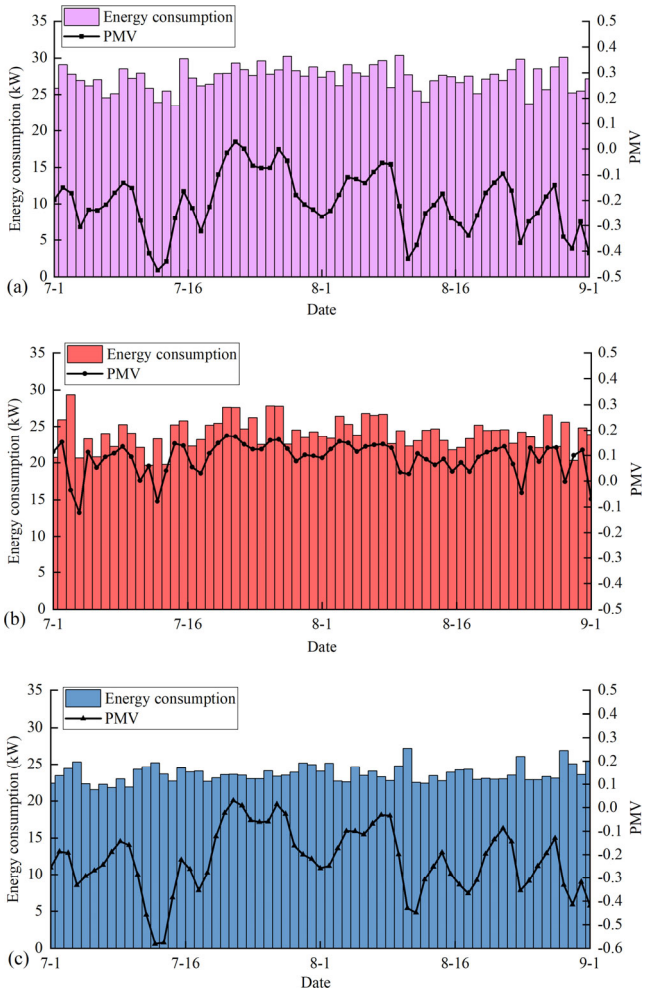

Fig. 15 The daily energy demand and average PMV of three control strategies in Chengdu: (a) Strategy 1, (b) Strategy 2, and (c) Strategy 3

operation of RFCSs (Gaetani et al. 2016). This study utilized a fixed personnel schedule, widely used in simulations. However, static occupancy modeling is not always appropriate due to the influence of indoor load variations and simulation errors (Liu et al. 2023). Further study will consider the use of more realistic occupancy patterns that reflect indoor disturbances more objectively to simulate a reasonable control of the system and improve the simulation accuracy. Furthermore, we used limited comparison parameters, and future research efforts should consider assigning weights to multiple parameters in different climate zones.

5 Conclusion

This study conducted a simulation of RFCS in residential buildings in five climate zones in China. Three conventional control strategies were assessed: variable water temperature control, variable air volume control and direct-ground source cooling. Multi-criteria evaluation was used to rank the three

control strategies. The strategies' application potential were analyzed. The following results are obtained:

The RFCS exhibited superior results in various climate zones. Strategy 2 provided the most favorable indoor thermal comfort, and the number of hours exceeding thermal comfort accounted for 3% of the total simulation time. In contrast, Strategy 3 had the least favorable indoor thermal environment. The indoor thermal environment could be improved by controlling the condensation risk of the RFCS, making it more suitable for residential buildings. The outdoor climate and the control strategy affected the condensation risk of radiant floor system. The condensation risk is the largest in the HSWW zone, followed by the HSCW and cold zones. Therefore, integrating floor temperature control and ventilation system control can effectively reduce the risk of condensation on radiant floor surfaces. The energy consumption of Strategy 1 was 19%–27% higher than that of Strategy 3, which had the lowest energy consumption. In practical applications, climatic conditions and regional electricity prices affected the electricity cost of the RFCSs.

The thermal comfort, condensation risk, energy consumption and carbon emissions of the control strategies were comprehensively compared. The performance of the direct-ground cooling source system was better in the HSWW zone, whereas the variable air volume strategy is recommended in the SC and Temperate zones. The variable water temperature control strategy did not perform as well as the other strategies and required need to be further optimization. During the initial stage of building design, it is crucial to prioritize and allocate suitable indicators during building design to guide the control strategy selection for RFCSs.

Acknowledgements

This work was funded by the Natural Science Foundation of Shandong Province (ZR2021ME199, ZR2021ME237) and the Support Plan for Outstanding Youth Innovation Team in Colleges and Universities of Shandong Province (2019KJG005). This work was also supported by the Plan of Introduction and Cultivation for Young Innovative Talents in Colleges and Universities of Shandong Province, and Funding for Domestic Visiting Scholars at Shandong Jianzhu University.

Declaration of competing interest

The authors have no competing interests to declare that are relevant to the content of this article.

Author contribution statement

Mengying Cui: investigation, methodology, data curation, modeling, writing, and original draft. Yang Song: investigation, data curation. Yudong Mao: investigation, data curation, writing. Kaimin Yang: data curation, modeling, writing. Jiying Liu: supervision, conceptualization, methodology, funding, review and editing. Zhe Tian: supervision, conceptualization, methodology, review and editing.

References

Abdel-Mawla MA, Hassan MA, Khalil A (2022). Impact of placement and design of phase change materials in thermally activated buildings. *Journal of Energy Storage*, 56: 105886.

Arghand T, Javed S, Trüschel A, et al. (2021). A comparative study on borehole heat exchanger size for direct ground coupled cooling systems using active chilled beams and TABS. *Energy and Buildings*, 240: 110874.

ASHRAE (2014). ASHRAE Guideline 14-2014. Measurement of Energy, Demand, and Water Saving. Atlanta, GA, USA: American Society of Heating, Refrigerating and Air-Conditioning Engineers.

Bean R, Olesen BW, Kim KW (2010). History of radiant heating & cooling systems: Part 2. *ASHRAE Journal*, 52(2): 50–55.

Chandrashekar R, Kumar B (2022). Experimental investigation on energy saving potential for thermally activated buildings integrated with the active cooling system. *Energy Sources, Part A: Recovery, Utilization, and Environmental Effects*, 44: 7585–7597.

Cui M, Liu J, Kim MK, et al. (2023). Application potential analysis of different control strategies for radiant floor cooling systems in office buildings in different climate zones of China. *Energy and Buildings*, 282: 112772.

Delmastro C, Martinez-Gordon R, Lane K, et al. (2022). Space Cooling. Available at https://www.iea.org/energy-system/buildings/space-cooling.

Gaetani I, Hoes P-J, Hensen JLM (2016). Occupant behavior in building energy simulation: Towards a fit-for-purpose modeling strategy. *Energy and Buildings*, 121: 188–204.

Gwerder M, Tödtli J, Lehmann B, et al. (2009). Control of thermally activated building systems (TABS) in intermittent operation with pulse width modulation. *Applied Energy*, 86: 1606–1616.

Hou J, Cao M, Liu P (2018). Development and utilization of geothermal energy in China: Current practices and future strategies. *Renewable Energy*, 125: 401–412.

Hu R, Niu JL (2012). A review of the application of radiant cooling & heating systems in Mainland China. *Energy and Buildings*, 52: 11–19.

Joe J, Karava P, Hou X, et al. (2018). A distributed approach to model-predictive control of radiant comfort delivery systems in office spaces with localized thermal environments. *Energy and Buildings*, 175: 173–188.

Kalz DE, Wienold J, Fischer M, et al. (2010). Novel heating and cooling concept employing rainwater cisterns and thermo-active building systems for a residential building. *Applied Energy*, 87: 650–660.

Kang Z, Peng X, Cheng X, et al. (2017). Analysis of condensation and thermal comfort of two kinds of compound radiant cooling air conditioning systems based on displacement ventilation. *Procedia Engineering*, 205: 1529–1534.

Lehmann B, Dorer V, Gwerder M, et al. (2011). Thermally activated building systems (TABS): Energy efficiency as a function of control strategy, hydronic circuit topology and (cold) generation system. *Applied Energy*, 88: 180–191.

Li Y, Niu F, Qian D, et al. (2018). Nationwide energy saving analysis of radiant floor system for commercial buildings. In: Proceedings of 2018 ASHRAE Annual Conference, Houston, USA.

Lim J-H, Jo J-H, Kim Y-Y, et al. (2006). Application of the control methods for radiant floor cooling system in residential buildings. *Building and Environment*, 41: 60–73.

Liu J, Ren J, Zhang L, et al. (2019). Optimization of Control Strategies for the Radiant Floor Cooling System Combined with Displacement Ventilation: A Case study of an Office Building in Jinan, China. *International Journal of Architectural Engineering Technology*, 6: 33–48.

Liu X, Hu S, Yan D (2023). A statistical quantitative analysis of the correlations between socio-demographic characteristics and household occupancy patterns in residential buildings in China. *Energy and Buildings*, 284: 112842.

MOHURD (2012). JGJ 142-2012. Technical Specification for Radiant Heating and Cooling. Ministry of Housing and Urban-Rural Development of China. Beijing: China Architecture & Building Press. (in Chinese)

MOHURD (2018). JGJ/T 440-2018. Technical Standard for Residential Outdoor Air System. Ministry of Housing and Urban-Rural Development of China. Beijing: China Architecture & Building Press. (in Chinese)

MOHURD (2019). GB/T 51366-2019. Building Carbon Emission Calculation Standard. Ministry of Housing and Urban-Rural Development of China. Beijing: China Architecture & Building Press. (in Chinese)

MOHURD (2021). GB 55015-2021. General Code for Energy Efficiency and Renewable Energy Application in Buildings. Ministry of Housing and Urban-Rural Development of China. Beijing: China Architecture & Building Press. (in Chinese)

Ning B, Schiavon S, Bauman FS (2017). A novel classification scheme for design and control of radiant system based on thermal response time. *Energy and Buildings*, 137: 38–45.

Oxizidis S, Papadopoulos AM (2013). Performance of radiant cooling surfaces with respect to energy consumption and thermal comfort. *Energy and Buildings*, 57: 199–209.

Ren J, Liu J, Zhou S, et al. (2022a). Experimental study on control strategies of radiant floor cooling system with direct-ground cooling source and displacement ventilation system: A case study in an office building. *Energy*, 239: 122410.

Ren J, Liu J, Zhou S, et al. (2022b). Developing a collaborative control strategy of a combined radiant floor cooling and ventilation system: A PMV-based model. *Journal of Building Engineering*, 54: 104648.

Rhee KN, Olesen BW, Kim KW (2017). Ten questions about radiant heating and cooling systems. *Building and Environment*, 112: 367–381.

Salvalai G, Pfafferott J, Sesana MM (2013). Assessing energy and thermal comfort of different low-energy cooling concepts for non-residential buildings. *Energy Conversion and Management*, 76: 332–341.

Schmelas M, Feldmann T, Bollin E (2015). Adaptive predictive control of thermo-active building systems (TABS) based on a multiple regression algorithm. *Energy and Buildings*, 103: 14–28.

Schmelas M, Feldmann T, Wellnitz P, et al. (2016). Adaptive predictive control of thermo-active building systems (TABS) based on a multiple regression algorithm: First practical test. *Energy and Buildings*, 129: 367–377.

Schmelas M, Feldmann T, Bollin E (2017). Savings through the use of adaptive predictive control of thermo-active building systems (TABS): A case study. *Applied Energy*, 199: 294–309.

Shahrestani M, Yao R, Cook GK, et al. (2012). Decision making for HVAC&R system selection for a typical office building in the UK. *ASHRAE Transactions*, 118(2): 222–229.

Srivastava P, Khan Y, Bhandari M, et al. (2018). Calibrated simulation analysis for integration of evaporative cooling and radiant cooling system for different Indian climatic zones. *Journal of Building Engineering*, 19: 561–572.

Sui X, Wang H, Qu M, et al. (2020). Thermal response characteristics of intermittently cooled room with tube-embedded cooling slab and optimization of intermittent control. *Energies*, 13: 1568.

Tian Z, Love JA (2009). Energy performance optimization of radiant slab cooling using building simulation and field measurements. *Energy and Buildings*, 41: 320–330.

Vivek T, Balaji K (2023). Heat transfer and thermal comfort analysis of thermally activated building system in warm and humid climate–A case study in an educational building. *International Journal of Thermal Sciences*, 183: 107883.

Zakula T, Armstrong PR, Norford L (2015). Advanced cooling technology with thermally activated building surfaces and model predictive control. *Energy and Buildings*, 86: 640–650.

Zarrella A, De Carli M, Peretti C (2014). Radiant floor cooling coupled with dehumidification systems in residential buildings: A simulation-based analysis. *Energy Conversion and Management*, 85: 254–263.

Zhang F, Guo HA, Liu Z, Zhang G (2021). A critical review of the research about radiant cooling systems in China. *Energy and Buildings*, 235: 110756.

Zhao K, Liu X, Jiang Y (2016). Application of radiant floor cooling in large space buildings—A review. *Renewable and Sustainable Energy Reviews*, 55: 1083–1096.

Zhou X, Liu Y, Zhang J, et al. (2022). Radiant asymmetric thermal comfort evaluation for floor cooling system–A field study in office building. *Energy and Buildings*, 260: 111917.

Zhu X, Liu J, Zhu X, et al. (2022). Experimental study on operating characteristic of a combined radiant floor and fan coil cooling system in a high humidity environment. *Buildings*, 12: 499.